ACS APPLIED MATERIALS & INTERFACES

Research Article

www.acsami.org

CuO Nanoparticles from the Strongly Hydrated Ionic Liquid Precursor (ILP) Tetrabutylammonium Hydroxide: Evaluation of the Ethanol Sensing Activity

Andreas Taubert,*[,†,‡] Franziska Stange,[†] Zhonghao Li,[§] Mathias Junginger,[†] Christina Günter,[⊥] Mike Neumann,[†] and Alwin Friedrich[†]

[†]Institute of Chemistry and [⊥]Institute of Earth and Environmental Sciences, University of Potsdam, D-14476 Potsdam, Germany

[‡]Max Planck Institute of Colloids and Interfaces, D-14476 Potsdam, Germany

[§]School of Materials Science and Engineering, Shandong University, Jinan 250012, P.R. China

Supporting Information

ABSTRACT: The sensing potential of CuO nanoparticles synthesized via precipitation from a water/ionic liquid precursor (ILP) mixture was investigated. The particles have a moderate surface area of 66 m^2/g after synthesis, which decreases upon thermal treatment to below 5 m^2/g. Transmission electron microscopy confirms crystal growth upon annealing, likely due to sintering effects. The as-synthesized particles can be used for ethanol sensing. The respective sensors show fast response and recovery times of below 10 s and responses greater than 2.3 at 100 ppm of ethanol at 200 °C, which is higher than any CuO-based ethanol sensor described so far.

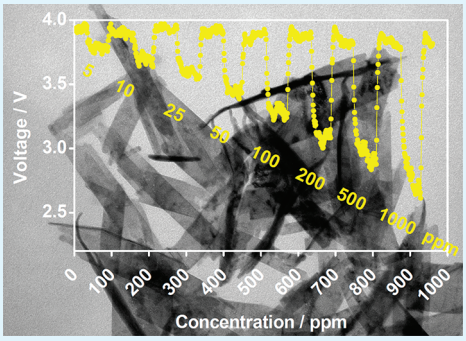

KEYWORDS: *ionic liquids, ionic liquid precursors, tetrabutylammonium hydroxide, nanoparticles, CuO, gas sensing*

INTRODUCTION

Ionic liquids (ILs) are probably among the most actively researched compounds of the recent past. Their interesting chemical and physical properties such as high solubilizing power and low vapor pressure have attracted interest for use in chemical transformations. Among others, ILs have been used for the synthesis of inorganic nanoparticles or solid state materials, occasionally with quite surprising results.[1−5]

The IL tetrabutylammonium hydroxide (TBAH), which is commercially available in a strongly hydrated form, is a viable precursor for the synthesis of a number of useful metal oxide or hydroxide nanoparticles[6,7] and the water content of TBAH dramatically affects the outcome of the particle synthesis.[8] Among others, CuO nanoparticles have successfully been synthesized from TBAH. CuO particle growth proceeds via rod- or fiberlike $Cu(OH)_2$ intermediates, which rapidly transform into CuO.[7] A similar CuO precipitate has subsequently been made by Mudring and co-workers using a process in 1-butyl-3-methylimidazolium bis(trifluoromethylsulfonyl)-imide [Bmim][NTf_2].[9]

A number of other CuO synthesis protocols from solution have been reported as well. Xia et al. have made flowerlike and "peachstone" CuO.[10,11] The latter appear to form via oriented aggregation of nanoparticles into 2D sheets and 3D objects in 1-octyl-3-methylimidazolium trifluoroacetate [Omim][TFA].[11] Li et al. synthesized Cu_2O nanoparticles with high photocatalytic activity using 1-n-butyl-3-methylimidazolium tetrafluoroborate [Bmim][BF_4] as an additive in the reaction mixture.[12] Zhu et al. have shown that the formation of CuO, Cu_2O, or Cu nanoparticles can be controlled by adjusting the [Bmim][BF_4] concentration in the reaction mixture.[13] CuO morphology adjustment by further variation of reaction conditions has also been reported.[14−17]

CuO is a p-type semiconductor with a narrow bulk band gap of 1.2 eV.[18] It is interesting for a number of technologically and commercially interesting applications such as water treatment[19−27] or heterogeneous catalysis.[28−43] In the recent past, CuO nanoparticle-catalyzed reactions have attracted increasing interest.[44−49] Besides catalysis, gas sensors based on copper oxides have also been studied.[50−54] As the synthesis of CuO nanoparticles from TBAH is fast (<10 min) and the yields are high,[6,7] the approach may be suitable for the large scale synthesis of CuO nanoparticles for a variety of applications, including sensing.

The current article therefore evaluates three so far unknown parameters of these CuO nanoparticles: (i) the surface area, (ii) the thermal stability, and (iii) the sensing efficiency using ethanol as an initial model. The thermal stability is important because thermally induced decomposition or sintering of the nanoparticles must be avoided for reliable long-term sensing

Received: October 17, 2011
Accepted: January 19, 2012
Published: January 19, 2012

   dx.doi.org/10.1021/am201427q | ACS Appl. Mater. Interfaces 2012, 4, 791−795

activity. If the processing temperatures during sensor preparation are too high, this may for example result in a decreasing surface area even before the sensor is put to operation for the first time. This may yield a bad or unreliable sensor. Likewise, if the operation temperature is too high, the sensor will initially work, but rapidly degrade and quickly become useless. The goal of the current study is therefore to establish optimal temperature windows for sensor preparation and operation. Indeed, the data demonstrate that the CuO nanoparticles obtained via our process can be processed up to 300 °C and have an ideal operation temperature of ca. 200 °C. Moreover, the data demonstrate that the sensors based on our CuO nanoparticles are the most sensitive ethanol sensor based on CuO known to date.

EXPERIMENTAL SECTION

Materials. Copper(II) acetate monohydrate (≥98%, Alfa Aesar), tetrabutylammonium hydroxide 30-hydrate (TBAH, ≥ 98%, Sigma-Aldrich), ethanol (≥99.8%, 1% methylethylketone, Roth), ethanol (p.a., VWR), and methanol (analytical grade, Merck) were used without further purification.

Synthesis. CuO particles were synthesized as published.[6,7] Annealing was done in a Linn High Therm LM 312.07 oven at 300, 500, 700, and 900 °C in air for 2 h.

Characterization. Elemental analysis was done on a Vario EL III analyzer. IR spectra were recorded on a Thermo-Nicolet Nexus FTIR in transmission (KBr pellet) mode. Spectra were recorded between 4000 and 400 cm^{-1} with a resolution of 4 cm^{-1} and 32 scans per spectrum. UV/vis spectra were recorded on a Kontron Uvikon Spectrophotometer 930 from 200 to 800 nm with 0.5 nm resolution. Thermogravimetric analysis was done on a Linseis L 81 thermal balance in air from 25 to 800 °C at 10 K/min. BET analysis was done on a Quantachrome Quadrasorb 1 at 77 K. X-ray diffraction was done on a Siemens D5005 (Bragg–Brentano theta–theta geometry) from 3 to 70° 2θ. X-ray wavelength was 1.5408 Å (CuK_α). Data were analyzed as described previously.[55] Transmission electron microscopy was done on a Philips CM100 operated at 80 kV. Prior to imaging, particles were deposited on pioloform-coated copper grids from a suspension in water.

Gas Sensing. Ethanol sensing of the CuO powders was investigated with a WS-30A static gas-sensing system (Weisheng Electronics Co. Ltd., Henan, P.R. China). Sensor response was studied in a sealed PMMA test chamber (18 dm^3) with a gas inlet and outlet. Different concentrations of test gases were obtained by dilution with fresh dry air. The test gas (ethanol) was injected into the test chamber through an injection hole and the sensor voltage was measured vs time until it attained a constant value. Before repeat experiments, the chamber was purged with fresh air (ca. 30% relative humidity).

The gas sensor is a side-heated type and was made as follows. CuO powders were mixed with ethanol in an agate mortar to form the gas-sensing paste. The paste was cast on a ceramic tube with a pair of Pt wires on Au electrodes. A Ni–Cr wire inserted into the ceramic tube (Figure 1) was used for heating. Temperature was automatically

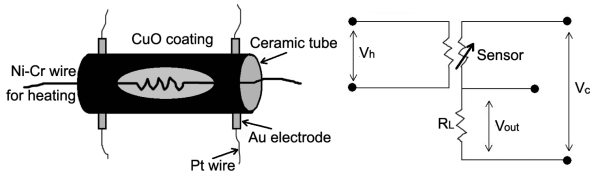

Figure 1. Experimental setup for ethanol sensing.

controlled by the external controller. The sensor performance was obtained from the V_{out} value of R_L that cascades R_s (the resistance of the gas sensor), Figure 1.

All gas sensors were aged at 300 °C for 10 h to improve their stability. In our experiment, R_L = 1 MΩ, V_c = 5 V, the voltages in the figures are V_{out}, so $R_a(R_g) = R_L(V_c - V_{out})/V_{out}$. Two different definitions of sensor response are commonly used: relative resistance variation ($S = (R_g - R_a)/R_a$) or resistance ratio ($S = R_g/R_a$). R_a is the resistance in dry air and R_g is the resistance of dry gas mixed with the analyte gas (ethanol). Here, we used the resistance ratio ($S = R_g/R_a$) to quantify the sensor response. All gas-sensing results were obtained in the static state and with dry air background; the real-time response curves were obtained from the same device.

RESULTS

1. Materials. The importance of thermal stability of the nanoparticles for sensor preparation and operation has been stated in the Introduction. To evaluate the thermal stability, we subjected CuO particles to heat treatments up to 900 °C. IR and UV/vis spectra (see Figure S1 in the Supporting Information) do not show distinct changes with temperature. All features can be assigned to CuO and the spectra will therefore not be discussed any further. X-ray diffraction (see Figure S2 in the Supporting Information) shows that in all cases (as-prepared and calcined), single-phase CuO (monoclinic tenorite, JCPDS 41–0254D) is obtained, consistent with previous reports.[6,7]

Figure 2 shows transmission electron microscopy (TEM) images of the as-prepared and the calcined samples. The as-prepared particles are identical to earlier reports[6,7] and have a size of ca. 50 to 100 nm with a broad size distribution. Samples calcined at 300 and 500 °C still show a platy to rodlike particle morphology and are electron-transparent. The samples calcined between 300 and 700 °C increasingly collapse and show signs of sintering, such as rounded edges, and a much less pronounced electron transparency. Samples calcined at 900 °C, surprisingly, show small particles with diameters on the order of 100 nm. TEM therefore demonstrates that there is a thermally induced collapse, which becomes most prominent at high temperatures.

Figure 3 shows further analytical data of the particles. Nitrogen sorption (Brunauer–Emmet–Teller model, BET)[57,58] shows that the surface area decreases roughly linearly with increasing treatment temperature from 66 m^2/g in the as-synthesized particles to below 5 m^2/g in the sample treated at 900 °C. This is consistent with TEM, which shows a drastic change in the particle morphology and a compaction of the samples with increasing calcination temperature. The initial surface area is similar to an earlier example of Cu_2O "nanoflowers",[12] but as the chemistry (CuO vs Cu_2O) is different, a further comparison is difficult.

Elemental analysis (EA) shows that already the treatment at 300 °C reduces the amount of C, H, and N to below 0.2%, which roughly represents the detection limit of the instrument. This is further confirmed by thermogravimetric analysis/differential thermal analysis (TGA/DTA), which finds a broad weight loss between room temperature and ca. 260 °C. The weight loss is assigned to desorption of water and other adsorbed molecules. This is confirmed by the endothermic DTA signal, which ranges up to ca. 500 °C. The breadth of the DTA signal suggests that there are additional sintering processes, which require thermal energy for activation. This is consistent with TEM, see above. The second endothermic signal above ca. 620 °C is most likely due to some thermal drift or a change in the sample. This is supported by control experiments and by a slight bump in the TGA data just when the DTA signal starts to drift at ca. 630 °C.

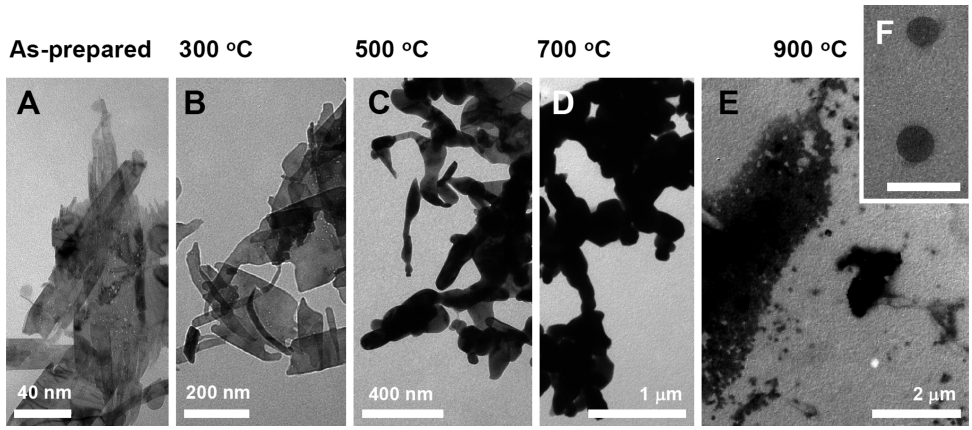

Figure 2. TEM images of an as-synthesized sample and samples calcined at 300, 500, 700, and 900 °C, respectively. Scale bar in (F) is 200 nm. For indexed XRD patterns, see Figure S2 in the Supporting Information. Size distributions of the annealed samples are difficult to determine, because of the heterogeneous particle shapes after thermal treatment. No size distributions but only size ranges are therefore given. Sizes of the as-prepared samples are given in ref 7.

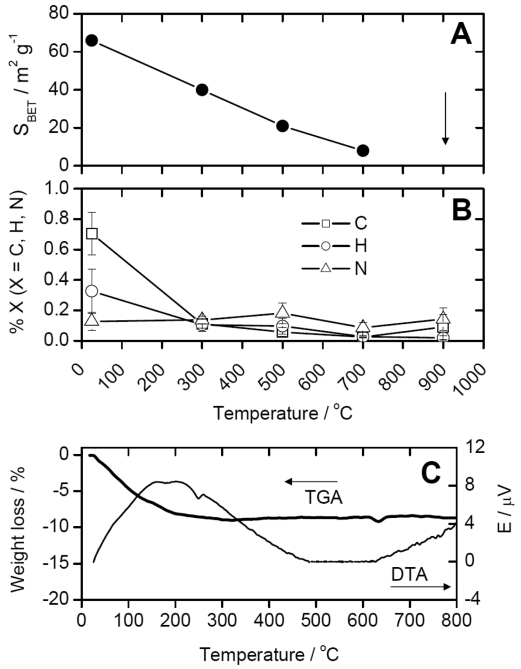

Figure 3. (A) Specific surface areas from BET analysis of the as-prepared and calcined samples. The surface area of the sample treated at 900 °C (arrow) is below the detection limit of the experimental setup (5 m^2/g). (B) Results of CHN analysis vs calcination temperature, (C) TGA (bold line) and DTA (thin line) data of as-prepared CuO.

As a result, EA and TGA/DTA confirm that the particles are essentially free of organic impurities (within the limits of the accuracy of the respective methods). XPS data, which would provide more accurate data, are not available, but IR spectra (see Figure S1 in the Supporting Information) do not indicate the presence of organic moieties. We therefore conclude that the resulting materials are single phase (aggregated) tenorite CuO nanoparticles. Overall, TGA/DTA, EA, and BET therefore confirm that annealing at 300 °C is suitable for preparing gas sensors: organic impurities are essentially removed, but the surface area is still acceptable for an application in gas sensing.

2. Sensing. Figure 4 shows representative ethanol sensing results. Ethanol was used as a first test case for our sensor, as there are data in the literature available for comparison.[50−54] To determine the optimum working temperature for our CuO-based sensors, the response to 100 ppm of ethanol was examined vs temperature, Figure 4A. The strongest response is observed at 200 °C; at higher temperatures the response decreases again. We have therefore performed all further experiments at 200 °C (this is not to be confused with the sensor annealing temperature during sensor fabrication, 300 °C; see Experimental Section for details).

Panels B and C in Figure 4 show the response/recovery curves and times of our CuO-based sensor to ethanol with concentrations between 5 and 1000 ppm at 200 °C. The as-prepared CuO nanostructures show a good response to ethanol; already at a low ethanol concentration of 5 ppm, the response is 1.22. The response further increases with increasing ethanol concentration, Figure 4D. For example, the response to 100 ppm ethanol is ca. 2.39, and the response times and recovery times are about 7 and 5 s, respectively. The response of our as-prepared CuO nanoparticles is therefore better than responses reported for CuO particles synthesized by calcination of $Cu(NO_3)_2$ at 400 °C (response of 1.6 for 100 ppm of ethanol)[59] and CuO nanowires synthesized by an oxidation reaction (response of 1.4 for 1000 ppm of ethanol).[60] To determine the accuracy and stability of our sensors, continuous tests with the same sensor at the same conditions were performed over extended periods of time. The respective data show a negligible sensitivity fluctuation, which demonstrates the good reproducibility and stability of our sensors.

DISCUSSION

The synthesis of single phase tenorite CuO nanoparticles from TBAH is a fast and efficient process providing rapid access to functional nanoparticles. The current article therefore evaluates the resulting nanoparticles for their use in gas sensing using ethanol as a model system. The surface area of the as-synthesized material is moderate at ca. 66 m^2/g; it decreases upon annealing (Figure 3). The decrease is most likely associated with a thermally induced densification, as is also evidenced by TEM (Figure 2). This clearly shows that sensor preparation must take place at low temperatures; otherwise the surface area (Figure 3) is too low for successful sensor operation.

However, if organic impurities must be removed, some temperature treatment is necessary, because the as-prepared

dx.doi.org/10.1021/am201427q | ACS Appl. Mater. Interfaces 2012, 4, 791−795

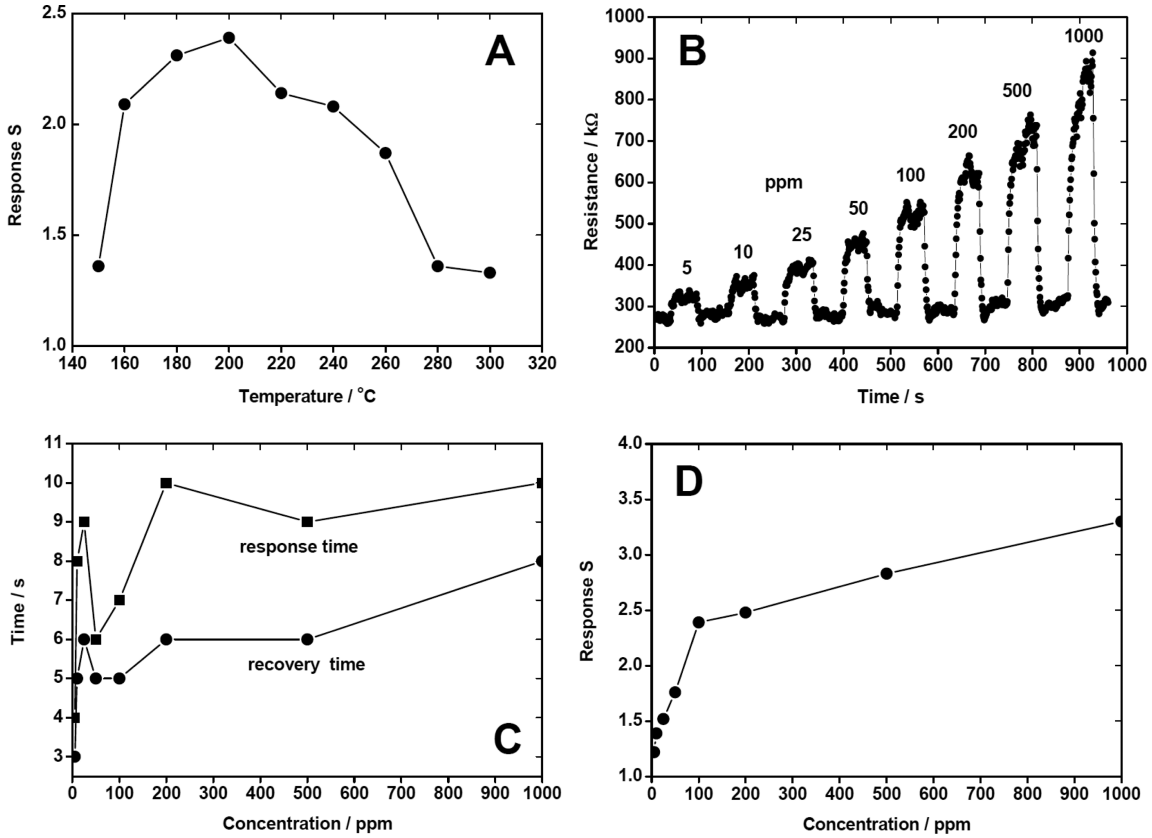

Figure 4. (A) Response vs working temperature for the CuO-based ethanol sensor and (B) the corresponding response/recovery curves at 200 °C. (C) Correlation between ethanol concentration and response/recovery times to ethanol at 200 °C. (D) Correlation between ethanol concentration and sensor response to ethanol at 200 °C.

CuO nanoparticles still contain 8−9% of organic matter (TGA and EA, Figure 3). The residual organic material decomposes below 300 °C and a sample preparation temperature of 250 to 300 °C is therefore a viable compromise between the highest possible surface area and the near-complete removal of organic contaminants. The samples treated at higher temperatures clearly have surface areas that are less attractive for sensor fabrication.

The sensors fabricated from the as-prepared CuO nanoparticles exhibit a good response of 2.39 at 200 °C (the optimum operating temperature) and high recovery rate (below 10 s). The current sensors are therefore more sensitive than other CuO-based ethanol sensors in the literature.[52,59−61] For example, the response of our as-prepared CuO nanoparticles is higher than the response of CuO nanoribbons synthesized via a surfactant-assisted hydrothermal route[52] and dandelion-like CuO microspheres synthesized from a $[Cu(pbbt)Cl_2]_2{\cdot}CH_3OH$ precursor;[61] both sensors have a response $S \approx 1$ from 5 to 1000 ppm ethanol. This is much lower than our result of $S > 2$. The reason for the decreasing response at higher temperatures in our sensors is probably due to a collapse of the nanoparticle architecture, as is evidenced in the TEM images, Figure 2.

The formation of the roughly spherical nanoparticles obtained at 900 °C is still under investigation. Such a particle size would in principle be useful due to the intrinsic high surface area of loose aggregates of these particles. Unfortunately, BET analysis (Figure 3) shows that the surface area of the resulting material is too small for successful sensor operation. We currently speculate that an additional process involving significant shrinking and densification (possibly controlled by the surface energy of the nanoparticles) is responsible for this new and somewhat surprising morphology. To further elucidate the process, high temperature in situ TEM or XRD would be necessary; this is currently not possible with our equipment and we can therefore not comment on the origin and mechanism of the process yielding the nanoparticles observed after annealing at 900 °C.

CONCLUSION

CuO is an interesting material for a variety of applications. The ease of nanoparticle synthesis and the short reaction times (<10 min.) should enable the mass production of CuO nanoparticles with relatively uniform shapes and sizes. Moreover, the reaction temperature in our process can be as low as 40 °C,[7] which is interesting from an economic point of view. The particles retain their properties up to ca. 300 °C. This is sufficient for constructing an ethanol sensor, which shows the best response at an operating temperature of 200 °C. The sensors will therefore further be evaluated for low temperature sensing of other important gases.

ASSOCIATED CONTENT

Supporting Information

IR and UV/vis spectra of all samples; indexed XRD patterns of all samples. This material is available free of charge via the Internet at http://pubs.acs.org.

AUTHOR INFORMATION

Corresponding Author

*E-mail: ataubert@uni-potsdam.de. Tel.: +49 (0) 331 977 5773.

Notes

The authors declare no competing financial interest.

■ ACKNOWLEDGMENTS

We thank B. Hannemann for EA, and A. Wilke and Dr. J. Weber for help with gas sorption. Financial support by the Deutsche Forschungsgemeinschaft (TA571/2-1, 3-1, 7-1), the University of Potsdam, and the MPI of Colloids and Interfaces (Colloid Chemistry Department) is gratefully acknowledged.

■ REFERENCES

(1) Antonietti, M.; Kuang, D.; Smarsly, B.; Zhou, Y. *Angew. Chem., Int. Ed.* **2004**, *43*, 4988.
(2) Morris, R. E. *Angew. Chem., Int. Ed.* **2008**, *47*, 443.
(3) Parnham, E. R.; Morris, R. E. *Acc. Chem. Res.* **2007**, *40*, 1005.
(4) Taubert, A. *Acta Chim. Slov.* **2005**, *52*, 183.
(5) Taubert, A.; Li, Z. *Dalton Trans.* **2007**, *7*, 723.
(6) Li, Z.; Rabu, P.; Strauch, P.; Mantion, A.; Taubert, A. *Chem.—Eur. J.* **2008**, *14*, 8409.
(7) Taubert, A.; Uhlmann, A.; Hedderich, A.; Kirchhoff, K. *Inorg. Chem.* **2008**, *47*, 10758.
(8) Zou, H.; Li, Z.; Luan, Y.; Mu, T.; Wang, Q.; Li, L.; Ge, J.; Chen, G. *Curr. Opin. Solid State Mater. Sci.* **2010**, *14*, 75.
(9) Alammar, T.; Birkner, A.; Mudring, A. V. *Eur. J. Inorg. Chem.* **2009**, 2765.
(10) Xia, J.; Li, H.; Luo, Z.; Shi, H.; Wang, K.; Shu, H.; Yan, Y. *J. Phys. Chem. Solids* **2009**, *70*, 1461.
(11) Xia, J.; Li, H.; Luo, Z.; Wang, K.; Yin, S.; Yan, Y. *Appl. Surf. Sci.* **2010**, *256*, 1871.
(12) Li, S. K.; Guo, X.; Wang, Y.; Huang, F. Z.; Shen, Y. H.; Wang, X. M.; Xie, A. J. *Dalton Trans.* **2011**, *40*, 6745.
(13) Zhu, L.; Chen, Y.; Sun, Y.; Cui, Y.; Liang, M.; Zhao, J.; Li, N. *Cryst. Res. Technol.* **2010**, *45*, 398.
(14) Xu, X.; Zhang, M.; Feng, J.; Zhang, M. *Mater. Lett.* **2008**, *62*, 2787.
(15) Zhang, M.; Xu, X.; Zhang, M. *J. Dispersion Sci. Technol.* **2008**, *29*, 508.
(16) Zhang, M.; Xu, X.; Zhang, M. *Mater. Lett.* **2008**, *62*, 385.
(17) Zhang, M.; Xu, X.; Zhao, Z.; Feng, J.; Zhang, M. *J. Dispersion Sci. Technol.* **2007**, *28*, 1223.
(18) Xiao, H.-M.; Fu, S.-Y.; Zhu, L.-P.; Li, Y.-Q.; Yang, G. *Eur. J. Inorg. Chem.* **2007**, 1966.
(19) Pintar, A.; Levec, J. *Chem. Eng. Sci.* **1992**, *47*, 2395.
(20) Drijvers, D.; Van Langenhove, H.; Beckers, M. *Water Res.* **1999**, *33*, 1187.
(21) Trapido, M.; Veressinina, Y.; Munter, R.; Kallas, J. *Ozone: Sci. Eng.* **2005**, *27*, 359.
(22) Fraga-Dubreuil, J.; Garcia-Serna, J.; Garcia-Verdugo, E.; Dudd, L. M.; Aird, G. R.; Thomas, W. B.; Poliakoff, M. *J. Supercrit. Fluids* **2006**, *39*, 220.
(23) Kim, J. K.; Martinez, F.; Metcalfe, I. S. *Catal. Today* **2007**, *124*, 224.
(24) Kim, J. K.; Metcalfe, I. S. *Chemosphere* **2007**, *69*, 689.
(25) Garg, A.; Mishra, I. M.; Chand, S. *Water Environ. Res.* **2008**, *80*, 136.
(26) Nezamzadeh-Ejhieh, A.; Hushmandrad, S. *Appl. Catal., A* **2010**, *388*, 149.
(27) Zhang, G.; Wang, S.; Zhao, S.; Fu, L.; Chen, G.; Yang, F. *Appl. Catal., B* **2011**, *106*, 370.
(28) Glander, S.; Ebert, I.; Scheve, J. *Z. Anorg. Allg. Chem.* **1974**, *405*, 257.
(29) Hassan, E. A.; Abd El-Salaam, K. M.; Said, A. A.; El-Awad, A. M. *Indian J. Chem., Sect. A: Inorg., Bio-inorg., Phys., Theor. Anal. Chem.* **1989**, *28A*, 860.
(30) Mantzavinos, D.; Hellenbrand, R.; Livingston, A. G.; Metcalfe, I. S. *Appl. Catal., B* **1996**, *7*, 379.
(31) Valatkevicius, P.; Krusinskaite, V.; Valinciute, V.; Valincius, V. *Surf. Coat. Technol.* **2003**, *174−175*, 1106.
(32) Pi, Y.; Ernst, M.; Schrotter, J. C. *Ozone: Sci. Eng.* **2003**, *25*, 393.
(33) Liu, X.; Liu, Y.; Li, X.; Xiang, S.; Zhang, Y.; Ying, P.; Wei, Z.; Li, C. *Appl. Catal., A* **2003**, *239*, 279.
(34) Toochinda, P.; Chuang, S. S. C.; Chi, Y. *Chem. Ind.* **2003**, *89*, 369.
(35) Bradu, C.; Avramescu, S.-M.; Udrea, I.; Mihalache, N. *Prog. Catal.* **2004**, *13*, 1.
(36) Choudhary, V. R.; Jha, R.; Chaudhari, N. K.; Jana, P. *Catal. Commun.* **2007**, *8*, 1556.
(37) Thakuria, H.; Borah, B. M.; Das, G. *J. Mol. Catal. A: Chem.* **2007**, *274*, 1.
(38) Basilio de Caland, L.; Santos, L. S. S.; Rodarte de Moura, C. V.; de Moura, E. M. *Catal. Lett.* **2009**, *128*, 392.
(39) Rahman, A. *Bull. Chem. React. Engin. Catal.* **2010**, *5*, 113.
(40) Kidwai, M.; Bhardwaj, S.; Poddar, R. *Beilstein. J. Org. Chem.* **2010**, 6 DOI: 10.3762/bjoc.6.35.
(41) Bandyopadhyay, P.; Sathe, M.; Prasad, G. K.; Sharma, P.; Kaushik, M. P. *J. Mol. Catal. A: Chem.* **2011**, *341*, 77.
(42) Ganesh Babu, S.; Karvembu, R. *Ind. Eng. Chem. Res.* **2011**, *50*, 9594.
(43) Sharma, S. K.; Bishopp, S. D.; Allen, C. L.; Lawrence, R.; Bamford, M. J.; Lapkin, A. A.; Plucinski, P.; Watson, R. J.; Williams, J. M. J. *Tetrahedron Lett.* **2011**, *52*, 4252.
(44) Zhang, J.; Zhang, Z.; Wang, Y.; Zheng, X.; Wang, Z. *Eur. J. Org. Chem.* **2008**, 5112.
(45) Rout, L.; Sen, T. K.; Punniyamurthy, T. *Angew. Chem., Int. Ed.* **2007**, *46*, 5583.
(46) Jammi, S.; Sakthivel, S.; Rout, L.; Mukherjee, T.; Mandal, S.; Mitra, R.; Saha, P.; Punniyamurthy, T. *J. Org. Chem.* **2009**, *47*, 1971.
(47) Rout, L.; Jammi, S.; Punniyamurthy, T. *Org. Lett.* **2007**, *9*, 3397.
(48) Pande, S.; Saha, A.; Jana, S.; Sarkar, S.; Basu, M.; Pradhan, M.; Kumar Sinha, A.; Saha, S.; Pal, A.; Pal, T. *Org. Lett.* **2008**, *10*, 5179.
(49) Prakash Reddy, V.; Vijay Kumar, A.; Swapna, K.; Rama Rao, K. *Org. Lett.* **2009**, *11*, 951.
(50) Zhang, J.; Liu, J.; Peng, Q.; Wang, X.; Li, Y. *Chem. Mater.* **2006**, *18*, 867.
(51) Chowdhuri, A.; Gupta, V.; Sreenivas, K.; Kumar, R.; Mozumdar, S.; Patanjali, P. K. *Appl. Phys. Lett.* **2004**, *84*, 1180.
(52) Gou, X.; Wang, G.; Yang, J.; Park, J.; Wexler, D. *J. Mater. Chem.* **2008**, *18*, 965.
(53) Barreca, D.; Gasparotto, A.; Maccato, C.; Tondello, E.; Lebedev, O. I.; Van Tendeloo, G. *Cryst. Growth Des.* **2009**, *9*, 2470.
(54) Barreca, D.; Comini, E.; Gasparotto, A.; Maccato, C.; Sada, C.; Sberveglieri, G.; Tondello, E. *Sens. Actuators, B* **2009**, *141*, 270.
(55) Taubert, A.; Kübel, C.; Martin, D. C. *J. Phys. Chem B* **2003**, *107*, 2660.
(56) Guinier, A. *X-ray Diffraction of Crystals, Imperfect Crystals and Amorphous Bodies*; Dover: New York, 1994.
(57) Brunauer, S.; Emmett, P. H.; Teller, E. *J. Am. Chem. Soc.* **1938**, *60*, 309.
(58) Polarz, S.; Smarsly, B. *J. Nanosci. Nanotechnol.* **2002**, *2*, 581.
(59) Li, J.-Y.; Xiong, S.; Xi, B.; Li, X.-G.; Qian, Y.-T. *Cryst. Growth Des.* **2009**, *9*, 4108.
(60) Raksa, P.; Gardchareon, A.; Chairuangsri, T.; Mangkorntong, P.; Mangkorntong, N.; Choopun, S. *Ceram. Int.* **2009**, *35*, 649.
(61) Mu, Y.; Yang, J.; Han, S.; Hou, H.; Fan, Y. *Mater. Lett.* **2010**, *64*, 1287.